

Terrain Slope Correction and Precise Registration of SAR Data for Forest Mapping and Monitoring

Z.-S. Zhou^a, E. Lehmann^a, X. Wu^a, P. Caccetta^a, S. McNeill^b, A. Mitchell^c, A. Milne^c, I. Tapley^c, K. Lowell^d

^aCSIRO Mathematics, Informatics and Statistics, Floreat, WA 6014, Australia
(zheng-shu.zhou, eric.lehmann, xiaoliang.wu, peter.caccetta)^a@csiro.au

^bLandcare Research, Lincoln, New Zealand – moneills@landcareresearch.co.nz

^cCooperative Research Centre for Spatial Information (CRC-SI), School of Biological, Earth and Environmental Sciences, The University of New South Wales, Sydney, NSW 2052, Australia – (a.mitchell, t.milne)^c@unsw.edu.au, hgciant@bigpond.net.au

^dCRC-SI, Department of Geomatics, University of Melbourne, Carlton, VIC 3052, Australia - klowell@unimelb.edu.au

Abstract - SAR data acquired over hilly terrain show geometric and radiometric distortions due to the side-looking configuration of the radar sensors. These effects usually lead to a distortion of the useful backscatter information related to land cover or bio-geophysical parameters. Post-processing approaches to remove such distortions are very important to broaden the application possibilities of radar remote sensing for land applications, especially in areas with significant terrain variation as can be found in many parts of Tasmania. Accurate orthorectification and terrain illumination correction for optical imagery have been well addressed in previous investigations. In this paper we present a new adaptation of algorithms which use the cosine of the surface tilt angles to more accurately correct for terrain slope illumination variations. We demonstrate the operational use of our approach using ALOS-PALSAR imagery. Critical to this task, and monitoring more generally, is accurate co-registration of data. To this end we provide a co-registration accuracy assessment of SAR data (including ALOS-PALSAR and RADARSAT-2 data) and compare it with Landsat imagery sourced from an operational forest monitoring system.

Keyword: geocoding, radiometric calibration, terrain slope correction, backscatter, forest mapping.

1. INTRODUCTION

In support of the GEO task on Forest Monitoring and Carbon Tracking, a project called the International Forest Carbon Initiative (IFCI) is conducting research on the complementary use of optical and SAR imagery for forest monitoring. A key component of the global initiative is to produce and make available a consistent time-series of annual, wall-to-wall forest change information products derived from an operational and interoperable methodology using complementary optical and SAR data. For the optical data, we build on work performed as part of the National Carbon Accounting System Land Cover Change Project (NCAS LCCP). The NCAS system makes use of time series of Landsat optical data so far. But for cloud affected regions, multi-temporal radar imagery provides improved prospects for forest change information thanks to the latest technological advancements of spaceborne SAR sensors in Earth observation.

As part of this global initiative, Australia has nominated Tasmania as one of the key test-sites in this GEO task. At this site, research is being conducted on globally-applicable methodology for the joint processing of remotely sensed optical and SAR data for forest change monitoring (Lehmann *et al.* 2011), combined with robust ground verification and accuracy assessment. A goal of the Tasmanian pilot is to produce forest

extent and extent change maps for the island, and to document their accuracies and limitations. Currently, the CSIRO, in collaboration with the CRCSI, is developing a credible remote sensing methodology and operational processing methods to transform the raw data into final products for forest mapping.

In this article we will focus on the issues of radiometric terrain corrections of SAR imagery and co-registration accuracy of multi-temporal images. We will investigate and demonstrate the suitability of a modified terrain slope correction for ALOS-PALSAR data over a mountainous area for forest mapping and monitoring. Section 2 will give a review of the terrain slope correction. A modified approach using the cosine of the surface tilt angles shows a more accurate terrain slope correction compared to the earlier terrain illumination correction used for optical images, as demonstrated in a comparison of the correction results in Section 3. We will show co-registration accuracy issues of Landsat, ALOS-PALSAR and RADARSAT-2 images in Section 4.

2. METHODOLOGY

Before SAR images are used in any classification scheme to distinguish land cover classes, geometric and radiometric corrections are required to remove any systematic or other effects unrelated to the cover classes being sought. For radiometry, the dominant effect is due to the variation in ground surface area contributing to the backscatter of each pixel. Variable terrain height causes both geometric and radiometric distortions within most slant or ground range SAR image products. The calibration of SAR data to radar backscatters has been analysed by many previous studies. SAR backscatter is strongly dependent on the slope and aspect of the terrain. Usually, solutions for the correction of the geometric distortions are widely available in SAR software packages. But robust correction of the radiometric distortions caused by terrain slope effects is typically either unavailable or treated with simplistic solutions. The radiometric calibration of SAR imagery is a critical pre-processing step for considering the further classification processing based on absolute backscattering values.

2.1 Geometric Parameters and Notations

Geometric parameters are described for their influence on the variations of SAR backscatter intensities. The parameters defined for each ground surface patch of an image are as follows (Figure 1):

- α - the slope angle
- β - the aspect of slope
- γ - the azimuth angle of the sensor
- θ - the nominal incidence angle

φ - the local incidence angle
 ψ - the complementary to the smallest angle between the surface normal and the image plane
 u - the surface tilt angle in the range direction,
 v - the surface tilt angle in the azimuth direction
 σ^0 - the original backscatter
 σ_c^0 - the radar backscatter corrected for the local incidence angle φ

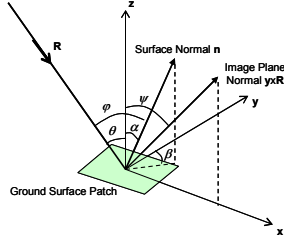


Figure 1. Scattering geometry of a tilted ground surface patch and its projection into the SAR image coordinates.

Some of these parameters, such as terrain slope and aspect values, are directly calculated from a digital elevation model (DEM) while others have to be calculated using the imaging geometry model. The terrain slope parameters are calculated using an estimation of the gradients in the two directions of the coordinate plane of the DEM. A 3-by-3 pixel window is usually used to calculate the gradients for the centre pixel. The local incidence angle φ is defined as the angle between the local surface normal and the look vector of the incident radar waves. The range component of the local incidence angle $\theta + u$ is used to determine regions of active layover in the digital elevation model, where u is defined as the angle between the vertical vector and the projection of the surface normal into the Doppler plane. The azimuth component of the local incidence angle v is defined as the angle between the local surface normal and the Doppler plane in a perpendicular direction to it.

2.2 Typical Terrain Slope Correction Models

Both theory and experiments point to certain expectations for the behaviour of SAR images of vegetation as a function of the radar incidence angle. Models of rough surface scattering are usually summarised into three categories:

A). Semi-empirical Formulations: which make use of relatively simple trigonometric functions to model the angular dependence without addressing the details of the interaction mechanisms involved such as

$$\sigma^0(\varphi) = \sigma^0 \cos^p(\varphi) \quad \text{for diffuse surfaces} \quad (1)$$

This is a simple backscattering model for vegetation-like media (Ulaby *et al.* 1986). Both σ^0 and p are polarisation dependent. When $p = 1$, the model means that the scattering coefficient (scattering per unit surface area) is dependent on $\cos \varphi$, which is the ratio of projected area (normal to the incoming rays) to the surface area. When $p = 2$, the model is based on Lambert's law for optics. Ulaby *et al.* pointed out that although either $p = 1$ or 2 seldom closely approximate the real scattering, sometimes $p=1$ or 2, or a value between 1 and 2 may be used to represent scattering from vegetation. Simulation results by Sun *et al.* (2002) showed a good agreement with this simple model to estimate σ^0 and p for both HH and HV polarisations.

B). Statistical Models: in which layers are represented by dielectric spaces containing random irregularities. Teillet *et al.* (1985) used a parameter C , which is a function of the regression slope a and intercept b from a linear relationship:

$$\sigma^0 = a \cdot \cos \varphi + b \quad (2)$$

$$C = b/a$$

Hence a so-called C-correction model is built based on the statistical regression as (Teillet *et al.* 1985):

$$\sigma_c^0 = \sigma^0 \frac{\cos \theta + C}{\cos \varphi + C} \quad (3)$$

where: σ_c^0 is the radar backscatter corrected for the local incidence angle φ , σ^0 is the backscatter before correction.

C). Geometrical Models: which use the sine of local incidence angle to correct the backscattering coefficient (van Zyl *et al.* 1993)

$$SCF = \frac{\sin \theta}{\sin(\theta + u) \cos v} \quad (4)$$

where SCF is the slope correction factor, $\theta + u$ the local radar incidence angle in the range direction, and v the surface tilt angle in the azimuth direction.

Another geometrical model is that of Kelldorfer *et al.* (1998), which used the local incidence angle φ to correct radiometric distortion due to the illumination areas.

$$\sigma_c^0 = \sigma^0 \frac{\sin \varphi}{\sin \theta} \quad (5)$$

2.3 A New Adaptation of the Slope Correction Approach

The SAR image products of JAXA use a sigma nought convention. This includes the PALSAR FBD SLC data. The calibrated radar backscatter of PALSAR data is retrieved as

$$\sigma^0 = \frac{I^2 + Q^2}{K} \quad (6)$$

where I and Q are the real and imaginary parts of the SLC product; and K is the calibration constant defined as -115.2 dB for FBD34.3 HH and -112.2 dB for FBD34.3 HV data acquired before 8 January 2009, and -115 dB for FBD34.3 HH/HV data acquired after 9 January 2009 (Shimada *et al.* 2009). The radar backscatter in beta nought is given as:

$$\beta^0 = \frac{\sigma^0}{\sin \theta} \quad (7)$$

where θ is the nominal incidence angle provided within the PALSAR product. Calculating the beta nought values as described above retrieves the radar backscatter values actually observed by the radar before the processor-induced ellipsoid-model nominal area values were applied to produce sigma nought estimates. A general calibration formula for σ^0 can take the form of (Ulander, 1996)

$$\sigma^0 = \beta^0 \cos \psi \quad (8)$$

$$\cos \psi = \sin \theta \cos \alpha + \cos \theta \sin \alpha \sin \beta \quad (9)$$

where ψ is the complementary to the smallest angle between the surface normal and the image plane, and α and β angles correspond to the slope and aspect angles of the surface relative to the vertical (z) and azimuth (y) directions, respectively. Slope and aspect were then generated from these elevations and used to calculate the local incidence angle for every pixel of the image as (Pairman *et al.* 1997):

$$\cos \varphi = \cos \theta \cos \alpha + \sin \theta \sin \alpha \cos(\gamma - \beta) \quad (10)$$

where φ is the local incidence angle, and γ is the azimuth angle of the sensor.

Ulander (1996) used the cosine of the angle between the normal of the slant range plane and the normal of the ground surface and surface tilted angles.

$$\sin(\theta + u)\cos v = \frac{\cos \psi}{\sqrt{1 + \left(\frac{\tan \alpha \cdot \sin \alpha \cdot \sin 2\beta}{2}\right)^2}} \quad (11)$$

where u is the surface tilt angle in the range direction, and v the surface tilt angle in the azimuth direction, as shown in Figure 2.

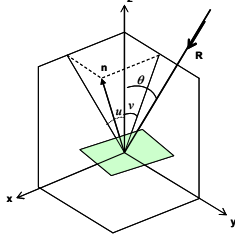


Figure 2. Surface tilt angles: u is the tilt angle in the range direction, and v the tilt angle in the azimuth direction.

A more accurate terrain slope correction by Eq. (11) was achieved while the worst-case ($\beta = 45^\circ + n \cdot 90^\circ$) calibration error is quite small for small slope angles and exceeds 1 dB only when the slope angle is greater than 60 degrees (Ulander, 1996).

There are three major land-cover classes in the study area: forest, agricultural land, and residential areas. Because the forest mapping is our primary objective, we define a modified terrain slope correction for tilted forest area as given below:

$$SCF = \sin(\theta + u)\cos v \quad (12)$$

$$\sigma_c^0 = SCF^q \cdot \beta^0 \quad (13)$$

where $q \approx 1/p$ according to Eq. (1), taking a value between 0.5 \sim 1 for the diffuse scattering. When a SAR image is acquired over a tilted terrain area, the surface slopes have two main effects on the SAR image backscatters. The first effect is a change of the radar cross section per unit image area, and the second effect is that polarisation states are also affected due to the azimuth slopes inducing the polarisation orientation changes. Since the L-band HH backscatter is more sensitive to slope (i.e., L-band waves have greater penetrating capability through canopy and therefore see more ground), it is used to estimate the local incidence angle φ . The SCF is then used to correct the HV image. Hence a simple analytical relationship is established between backscattering coefficients and incidence angle for both HH and HV images.

3. COMPARISON OF CORRECTION RESULTS

The PALSAR FBD (Fine-Beam Dual-pol) data are used to perform the comparison due to their suitable wavelength, scale and acquisition frequency. Geocoding is carried out using a 25m spacing Digital Elevation Model to correct for terrain and illumination effects resulting from the sidelooking geometry of SAR. This elevation model was generated from the interpolation of topographic contour data, and has a higher accuracy than global elevation models such as the SRTM or ASTER derived DEMs. Radiometric calibration is applied to allow for direct comparison of images acquired on different dates and/or with other SAR sensors. In earlier work carried out as a part of IFCI, we made use of the statistical model C-correction modified from a previous optical process to correct the PALSAR data. As shown below, the resulting images have some visible artefacts. As described in this paper, we also apply the proposed approach based on a semi-empirical forest scattering model and a geometric angular model. Figure 3 shows a comparison of an image before and after the

corrections, as well as the related correction coefficients. Moderate improvements of correction by the new method are observed while the previous one can be seen to over-correct the image. Figure 4 shows the spatial profiles of two lines, where the new approach shows a better correction.

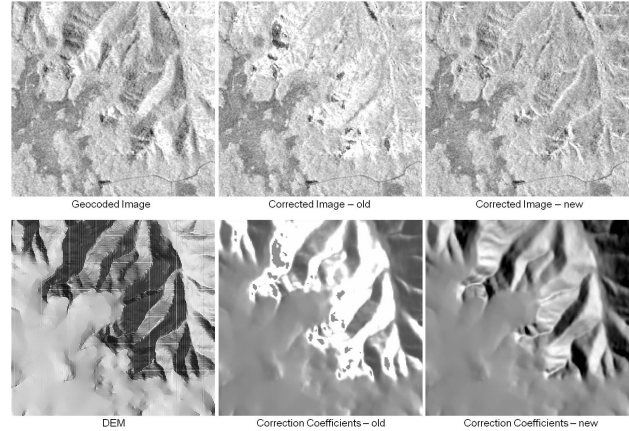


Figure 3. Comparison of terrain slope corrections by a method modified from C-correction for optical process and the new approach.

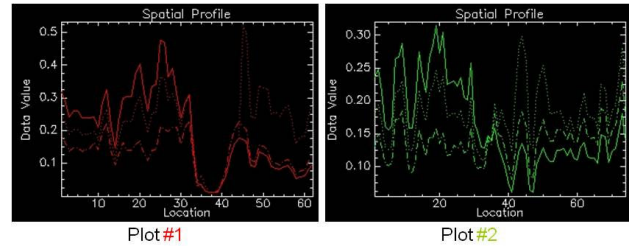


Figure 4. Spatial profiles of lines across terrain ridges for pre-correction (solid line), correction by C-correction (dotted line) and the new approach (dash-dot line).

Further improvements can be found by comparing the composite images (Red for HH and Green for HV) for both the early and new corrections, as shown in Figure 5. In the middle of the left image, there is a flaw for the HH image where some data is missing after correction possibly due to the regression applied to each band separately. This issue has been rectified by the new approach, as shown in the image on the right.

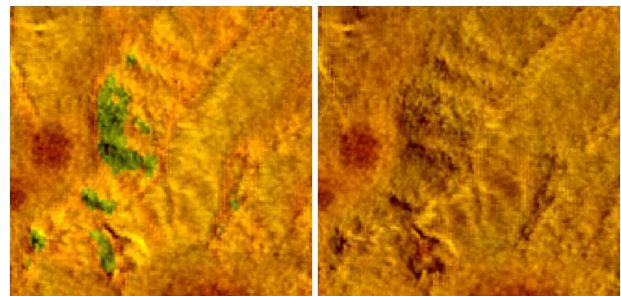


Figure 5. Comparison of old (Left) and new (Right) corrected images: Red-HH, Green-HV.

4. CO-REGISTRATION ACCURACY ASSESSMENT

For proper terrain slope correction, accurate geocoding and co-registration are essential. Otherwise displacements of the image cells will cause significant problems for the slope correction over the terrain ridges and valleys. Because optical image processing methodologies are well-established in the NCAS framework, co-registration accuracy of PALSAR data is assessed against the corresponding Landsat mosaic of

Tasmania. Overall there was a close correlation between the two datasets, with reduced accuracy in areas of steeper terrain in the south and also for neighbouring islands. The co-registration accuracy is tested using a cross-correlation technique to determine the shift between two datasets, given a set of manually chosen GCPs. Table 1 shows a sub-pixel co-registration accuracy for north-eastern Tasmania but an average difference of more than three pixels for south-western mountainous areas with displacements in more-or-less random directions. There could be two significant reasons for the poor co-registration results: difference of backscattering/reflection of landcovers acquired by radar and optical sensors, and lack of clear features for the cross-correlation in densely forested mountainous regions.

Table 1. Co-registration accuracy assessment of PALSAR data to Landsat imagery

Scene	RMS Errors in Row	RMS Errors in Column	Combined RMS Errors	Maximum Displacement	Displacement Orientation
NE Tas	0.54	0.60	0.86	1.90	random
SE Tas	0.50	1.19	1.18	2.31	random-NW
SW Tas	3.10	2.24	3.82	6.18	random

ALOS has highly accurate orbit and position parameters which should lead to the PALSAR imagery exhibiting a more reliable geometric accuracy. This has been assessed from the processed images by the following investigation. The co-registration accuracy of the PALSAR data was assessed against scenes of RADARSAT-2 data over northeast, northwest and southwest Tasmania, acquired in 2009. Because cross-pol images show more comparable features in forest areas, we chose RADARSAT-2 VH data and HV mosaic of PALSAR to check the correlation. Table 2 and Figure 6 present a comparison of the co-registration accuracies between the RADARSAT-2 and PALSAR images and their displacement orientations.

Table 2. Co-registration accuracy assessment of RADARSAT-2 data to PALSAR imagery

Scene	RMS Errors in Row	RMS Errors in Column	Combined RMS Errors	Maximum Displacement	Displacement Orientation
NE Tas	0.66	1.06	1.31	2.72	SE
NW Tas	0.82	1.35	1.61	3.14	SE
SW Tas	0.64	1.43	1.60	3.30	SE

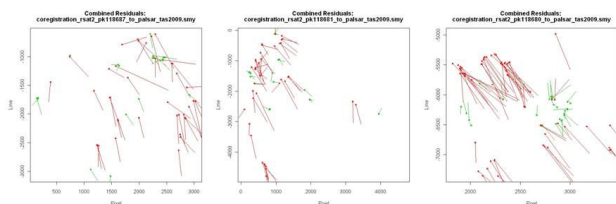


Figure 6. RMS Error displacements of co-registration of RADARSAT-2 and PALSAR images: NE (left), NW (middle) and SW (right) Tas.

Similar displacements are observed for all NE, NW and SW regions, with a north-western shift of about 1.5 pixels (25m pixel size) between the RADARSAT-2 data and PALSAR image (Figure 6). It shows consistent Root-Mean-Square (RMS) Errors for two types of images over the whole Tasmania. These results may be due to a systematic issue of two sensors. Further processing of the optical imagery is necessary to achieve a proper co-registration with respect to the PALSAR imagery. An independent test of all three datasets using ground control points from LiDAR survey will be worthy carrying out.

5. CONCLUSIONS

The radiometric calibration of SAR imagery is a critical pre-processing step for subsequent classification processing based on absolute backscatter values. In this paper, the radiometric terrain slope correction of SAR data has been reviewed. In

contrast to an earlier optical-based terrain illumination correction, a modified approach for SAR image correction over a mountainous area has been proposed. This method combines a semi-empirical forest scattering model and a geometric angular model using the cosine angle between the normal of the slant range plane and the normal of the ground surface associated with the surface tilted angles. Initial results have shown a better correction for PALSAR data at a test site. Improvements for both radiometric calibration and image consistency were observed. The following analysis for forest mapping application has been addressed in the paper of Lehmann *et al.* (2011).

In the past, people have only addressed the so-called "bulk effect correction" for terrain slope variation (Pairman *et al.* 1997), and others seem to follow the same route. The transformation using the covariance matrix is an additional factor for polarimetric SAR data correction (Schuler *et al.* 1999). However, we cannot implement it given that only dual-pol data are available. In the proposed method, we are effectively empirically fitting the net effect of the covariance matrix correction.

We have examined another critical issue for this wall-to-wall mapping project which is co-registration accuracy of multi-temporal data acquired by ALOS-PALSAR, RADARSAT-2 and Landsat. It was shown that it will be necessary to co-register other remote sensing data to the latest SAR images for precise geolocation accuracy.

REFERENCES

- Kellndorfer J., L. E. Pierce, M. C. Dobson, & F. T. Ulaby, 1998, "Toward Consistent Regional-to-Global-Scale Vegetation Characterization Using Orbital SAR Systems," *IEEE Trans. Geosci. Remote Sens.*, vol. 36, no. 5, pp. 1396–1411.
- Lehmann E., P. Caccetta, Z.-S. Zhou, A. Mitchell, I. Tapley, A. Milne, A. Held, K. Lowell, S. McNeill, 2011, "Forest Discrimination Analysis of Combined Landsat TM and ALOS-PALSAR Data," *Proc. International Symposium for Remote Sensing of the Environment*, Sydney, Australia
- Pairman D., S.E. Belliss and S. J. McNeill, 1997, "Terrain Influences on SAR Backscatter around Mt. Taranaki, New Zealand," *IEEE Trans. Geosci. Remote Sens.*, vol. 35, no. 4, pp. 924–932.
- Schuler D. L., J. S. Lee and T. L. Ainsworth, 1999, "Compensation of Terrain Azimuthal Slope Effects in Geophysical Parameter Studies using Polarimetric SAR Data," *Remote Sens. Environ.*, vol. 69, pp. 139–155, 1999.
- Shimada M., O. Isoguchi, T. Tadono, and K. Isono, 2009, "PLASAR Radiometric Calibration and Geometric Calibration," *IEEE Trans. Geosci. Remote Sens.*, vol. 47, pp. 3915–3932.
- Sun G., K. J. Ranson and V. I. Kharuk, 2002, "Radiometric Slope Correction for Forest Biomass Estimation from SAR Data in Western Sayani Mountains, Siberia," *Remote Sens. Environ.*, vol. 79, pp. 279–287.
- Teillet P.M., B. Guindon, J.F. Meunier and D.G. Goodenough, 1985, "Slope-Aspect Effects in Synthetic Aperture Radar Imagery," *Can. J. Remote Sensing*, vol. 11, no. 1, pp. 39–50.
- Ulaby F.T., R. K. Moore & A. K. Fung, 1982, "Microwave Remote Sensing, Active and Passive, vol. III". Norwood, MA: Artech House
- Ulander L.M.H., 1996, "Radiometric Slope Correction of Synthetic-Aperture Radar Images," *IEEE Trans. Geosci. Remote Sens.*, vol. 34, no. 5, pp. 1115–1122.
- van Zyl J.J., 1993, "The Effect of Topography on Radar Scattering from Vegetated Areas," *IEEE Trans. Geosci. Remote Sens.*, vol. 31, no. 1, pp. 153–160.